

# Atmospheric Chemistry of $n\text{-C}_x\text{F}_{2x+1}\text{CHO}$ ( $x = 1, 3, 4$ ): Reaction with Cl Atoms, OH Radicals and IR Spectra of $\text{C}_x\text{F}_{2x+1}\text{C}(\text{O})\text{O}_2\text{NO}_2$

M. P. Sulbaek Andersen and O. J. Nielsen

Department of Chemistry, University of Copenhagen, Universitetsparken 5, DK-2100 Copenhagen, Denmark

M. D. Hurley, J. C. Ball, and T. J. Wallington\*

Ford Motor Company, P. O. Box 2053, Dearborn, Michigan 48121-2053

J. E. Stevens

Department of Chemistry and Biochemistry, University of Detroit Mercy, 4001 West McNichols Road, P. O. Box 19900, Detroit, Michigan 48219-0900

J. W. Martin, D. A. Ellis, and S. A. Mabury

Department of Chemistry, 80 St. George Street, University of Toronto, Toronto, Ontario, Canada M5S 3H6

Received: January 23, 2004; In Final Form: March 15, 2004

Smog chamber/FTIR techniques were used to measure  $(\text{Cl} + n\text{-C}_x\text{F}_{2x+1}\text{CHO}, x = 1, 3, 4) = (2.1 \pm 0.5) \times 10^{-12}$  and  $k(\text{OH} + n\text{-C}_x\text{F}_{2x+1}\text{CHO}, x = 1, 3, 4) = (6.5 \pm 1.2) \times 10^{-13} \text{ cm}^3 \text{ molecule}^{-1} \text{ s}^{-1}$  in 700 Torr of  $\text{N}_2$ , or air, at  $296 \pm 2 \text{ K}$ . Cl-initiated oxidation of  $n\text{-C}_x\text{F}_{2x+1}\text{CHO}$  in the presence of NO in air diluent gave COF<sub>2</sub> in molar yields of  $91 \pm 11\%$ ,  $x = 1$ ;  $273 \pm 36\%$ ,  $x = 3$ ; and  $371 \pm 44\%$ ,  $x = 4$ . Small quantities (molar yields  $\leq 3\%$ ) of  $\text{CF}_3\text{ONO}_2$  and  $n\text{-C}_x\text{F}_{2x+1}\text{C}(\text{O})\text{O}_2\text{NO}_2$  were also observed. IR spectra of  $n\text{-C}_x\text{F}_{2x+1}\text{C}(\text{O})\text{O}_2\text{NO}_2$  ( $x = 1, 3, 4$ ) are reported. Results are discussed with respect to the atmospheric degradation of fluorinated aldehydes,  $\text{C}_x\text{F}_{2x+1}\text{CHO}$ .

## 1. Introduction

Concerns regarding the environmental impact of chlorofluorocarbon (CFC) release into the atmosphere have led to the replacement of CFCs in industrial processes and consumer products.

Hydrofluorocarbons (HFCs) and hydrochlorofluorocarbons (HCFCs) are two classes of compounds that have gained widespread use as CFC substitutes. Polyfluorinated alcohols are currently used in a variety of industrial products (paints, coatings, polymers, adhesives, waxes, polishes, electronic materials, and caulks<sup>1</sup>). Perfluorinated aldehydes are formed during the atmospheric oxidation of HFCs, HCFCs, and fluorinated alcohols.<sup>2</sup>

Long-chain perfluoroalkyl carboxylic acids (PFCAs,  $\text{C}_x\text{F}_{2x+1}\text{-COOH}$ , where  $x = 6\text{--}12$ ) have been observed recently in fish<sup>3,4</sup> and mammals<sup>5</sup> in a variety of locations around the world. PFCAs are not generally used directly in consumer or industrial materials, other than in aqueous film forming foams or as polymerization aids in fluoropolymer manufacture.<sup>6</sup> Thermolysis of fluoropolymers produces PFCAs; however, the magnitude of this source appears insufficient to account for the observed global environmental burden of these compounds.<sup>7</sup> The PFCAs observed in the environment are presumably the degradation products of precursor chemicals. However, the identity of the precursors and mechanism by which they are converted into PFCAs are unknown at the present time.

Perfluorinated aldehydes of the general formula  $\text{C}_x\text{F}_{2x+1}\text{CHO}$  have a molecular formula that is similar to that of perfluoroalkyl carboxylic acids. Atmospheric oxidation of perfluorinated

aldehydes offers a possible route to the formation of PFCAs. Unfortunately, there are few available data upon which to make a quantitative assessment of the contribution made by atmospheric oxidation of perfluorinated aldehydes to the observed budget of PFCAs. To remedy this situation, we have reported the results of an investigation into the atmospheric chemistry of  $\text{C}_2\text{F}_5\text{CHO}$ .<sup>8,9</sup> To expand upon this work, a study of the atmospheric chemistry of  $\text{CF}_3\text{CHO}$ ,  $n\text{-C}_3\text{F}_7\text{CHO}$ , and  $n\text{-C}_4\text{F}_9\text{CHO}$  was performed. Studies of fluorinated alcohols<sup>10</sup> and acids<sup>11</sup> suggest that  $n\text{-C}_3\text{F}_7\text{CHO}$  and  $n\text{-C}_4\text{F}_9\text{CHO}$  will serve as useful models with which to understand the degradation mechanism of long chain perfluoroaldehydes. Straight chain isomers  $n\text{-C}_3\text{F}_7\text{CHO}$  and  $n\text{-C}_4\text{F}_9\text{CHO}$  were studied in the present work. For simplicity, we will refer to these species as  $\text{C}_3\text{F}_7\text{CHO}$  and  $\text{C}_4\text{F}_9\text{CHO}$  in the rest of this article.

We have used smog chamber FTIR techniques to study the kinetics of reactions of Cl atoms and OH radicals with  $\text{C}_x\text{F}_{2x+1}\text{CHO}$  ( $x = 1, 3, 4$ ) and oxidation products of the Cl-initiated oxidation of  $\text{C}_x\text{F}_{2x+1}\text{CHO}$  in the presence of  $\text{NO}_x$ . Quantum mechanical calculations were employed to locate stable ground-state geometries for  $\text{CH}_3\text{C}(\text{O})\text{OONO}_2$  and  $\text{C}_x\text{F}_{2x+1}\text{C}(\text{O})\text{OONO}_2$  ( $x = 1\text{--}4$ ) and to calculate IR spectra for these molecules. Results are discussed with respect to the atmospheric chemistry and environmental impact of fluorinated organic compounds.

## 2. Experimental Section

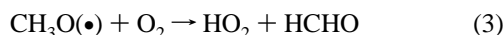
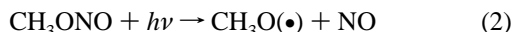
**2.1. Kinetic and Mechanistic Experiments.** The apparatus and experimental techniques used in this work have been described elsewhere.<sup>12,13</sup> Experiments were performed in a 140-L Pyrex reactor interfaced to a Mattson Sirius 100 FTIR spectrometer. The reactor was surrounded by 22 fluorescent

\* Corresponding author. E-mail: twalling@ford.com.

blacklamps (GE F15T8-BL), which were used to photochemically initiate the experiments. Chlorine atoms were produced by photolysis of molecular chlorine.



OH radicals were produced by photolysis of  $\text{CH}_3\text{ONO}$  in the presence of NO in air:



Reactant and product concentrations were monitored using *in situ* Fourier transform infrared spectroscopy. IR spectra were derived from 32 coadded interferograms with a spectral resolution of  $0.25 \text{ cm}^{-1}$  and an analytical path length of 27.1 m. Calibrated reference spectra were acquired by expanding known volumes of reference materials into the chamber. The vapor above liquid  $\text{CF}_3\text{C}(\text{O})\text{OH}$ ,  $\text{C}_3\text{F}_7\text{C}(\text{O})\text{OH}$ , and  $\text{C}_4\text{F}_9\text{C}(\text{O})\text{OH}$  contains monomers and dimers. Values of  $K_{\text{eq}}(\text{CF}_3\text{C}(\text{O})\text{OH}) = [\text{dimer}]/[\text{monomer}]^2 = 0.32 \pm 0.03 \text{ Torr}^{-1}$ ,  $K_{\text{eq}}(\text{C}_3\text{F}_7\text{C}(\text{O})\text{OH}) = 0.41 \pm 0.04 \text{ Torr}^{-1}$ , and  $K_{\text{eq}}(\text{C}_4\text{F}_9\text{C}(\text{O})\text{OH}) = 0.46 \pm 0.05 \text{ Torr}^{-1}$ <sup>11</sup> were used to correct for the presence of dimer (5–26% partial pressure) in the calibrated volumes. Analysis of the IR spectra was achieved through a process of spectral stripping in which small fractions of the reference spectrum were subtracted incrementally from the sample spectrum.

Samples of  $\text{C}_x\text{F}_{2x+1}\text{CHO}$  ( $x = 1, 3, 4$ ), were synthesized as described elsewhere<sup>8</sup> and purified by vacuum distillation. All other reactants were obtained from commercial sources at purities >99%. Ultrahigh purity air (total hydrocarbons < 0.1 ppm) and  $\text{O}_2$  (>99.994%) diluent gases were used as received. In smog chamber experiments, unwanted loss of reactants and products via photolysis and heterogeneous reactions has to be considered. Control experiments were performed in which product mixtures obtained after UV irradiation were allowed to stand in the dark in the chamber for 30 min. There was no observable (<2%) loss of reactants or products. Samples of  $\text{C}_x\text{F}_{2x+1}\text{CHO}$  or  $\text{C}_x\text{F}_{2x+1}\text{C}(\text{O})\text{OH}$  were subjected to UV irradiation in 700 Torr of air diluent for 15 min. There was no observable loss of  $\text{C}_x\text{F}_{2x+1}\text{CHO}$  or  $\text{C}_x\text{F}_{2x+1}\text{C}(\text{O})\text{OH}$ , suggesting that photolysis of these compounds is not significant in the present work.

**2.2. Computational Details.** Calculations were performed using the Gaussian 98 electronic structure package.<sup>14</sup> Geometry optimizations with the B3LYP/6-311G(d,p) method located stable ground-state geometries for  $\text{CH}_3\text{C}(\text{O})\text{OONO}_2$  and  $\text{C}_x\text{F}_{2x+1}\text{C}(\text{O})\text{OONO}_2$ . All optimizations were conducted in  $C_1$  symmetry. A subsequent B3LYP/6-311G(d,p) vibrational frequency calculation was used to derive an IR spectrum for each optimized geometry.

### 3. Results and Discussion

**3.1. Relative Rate Study of the Cl +  $\text{C}_x\text{F}_{2x+1}\text{CHO}$  ( $x = 1, 3, 4$ ) Reaction in 700 Torr of Air or Nitrogen.** The kinetics of reaction 5 were measured relative to reactions 6 and 7:

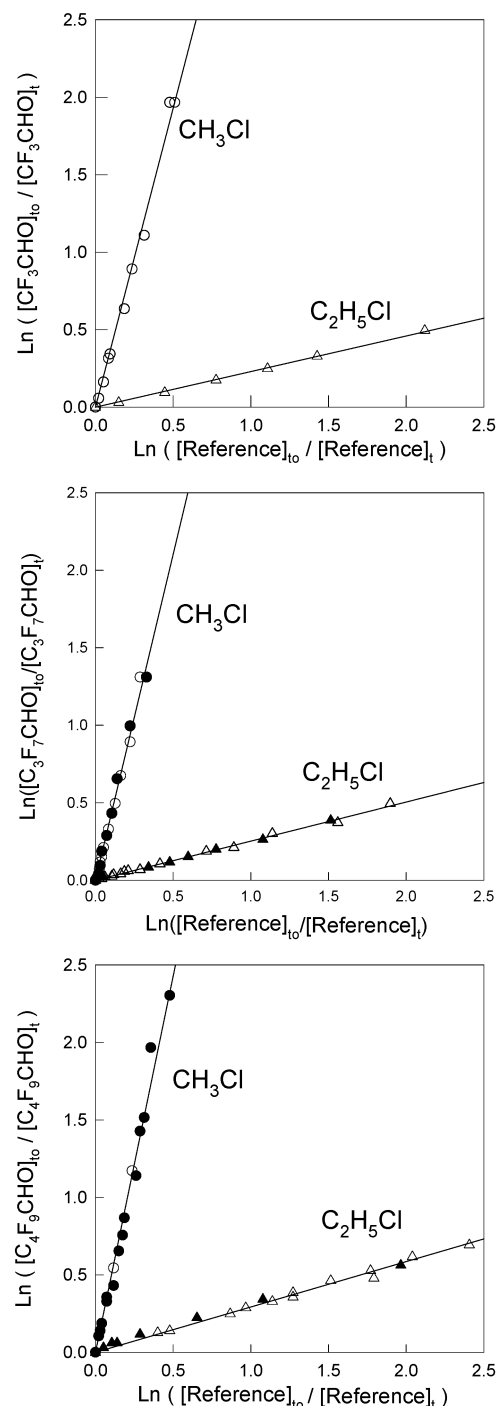
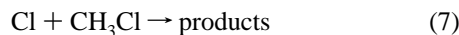
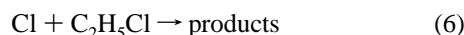
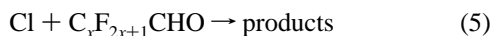


**Figure 1.** Decay of  $\text{C}_x\text{F}_{2x+1}\text{CHO}$  ( $x = 1, 3, 4$ ) versus  $\text{CH}_3\text{Cl}$  (circles) or  $\text{C}_2\text{H}_5\text{Cl}$  (triangles) in the presence of Cl atoms in 700 Torr of either air (solid symbols) or  $\text{N}_2$  (open symbols) diluent at  $296 \pm 2 \text{ K}$ .

Reaction mixtures consisted of 6.9–16.2 mTorr  $\text{C}_x\text{F}_{2x+1}\text{CHO}$ , 99.9–118 mTorr  $\text{Cl}_2$ , and 19.1–44.5 mTorr of either  $\text{C}_2\text{H}_5\text{Cl}$ , or  $\text{CH}_3\text{Cl}$ , in 700 Torr of either air, or  $\text{N}_2$ . The observed loss of  $\text{C}_x\text{F}_{2x+1}\text{CHO}$  versus that of the reference compounds in the presence of Cl atoms is shown in Figure 1. Linear least-squares analysis of the data in Figure 1 gives  $k_5/k_6 = 0.230 \pm 0.029$  and  $k_5/k_7 = 3.86 \pm 0.54$  for  $x = 1$ ,  $k_5/k_6 = 0.252 \pm 0.028$ , and  $k_5/k_7 = 4.21 \pm 0.44$  for  $x = 3$ , and  $k_5/k_6 = 0.293 \pm 0.030$ , and  $k_5/k_7 = 4.85 \pm 0.50$  for  $x = 4$ . Quoted uncertainties are two standard deviations from the linear regressions (forced through zero), together with our assessment of the uncertainties associated with the IR analysis of the reactant and reference concentrations. Using  $k_6 = 8.04 \times 10^{-12}$ ,<sup>15</sup> and  $k_7 = 4.8 \times$

$10^{-13}$ ,<sup>16</sup> we derive  $k_5 = (1.85 \pm 0.23)$  and  $(1.85 \pm 0.26) \times 10^{-12}$  for  $x = 1$ ,  $k_5 = (2.03 \pm 0.23)$  and  $(2.02 \pm 0.21) \times 10^{-12}$  for  $x = 3$ , and  $k_5 = (2.35 \pm 0.24)$  and  $(2.33 \pm 0.24) \times 10^{-12}$   $\text{cm}^3 \text{ molecule}^{-1} \text{ s}^{-1}$  for  $x = 4$ . Consistent results for the individual compounds were obtained using both references. Taking the average of the results obtained using the two different reference compounds together with error limits which encompass the extremes of the individual determinations, we arrive at values of  $k_5 = (1.85 \pm 0.26) \times 10^{-12}$  for  $x = 1$ ,  $(2.03 \pm 0.23) \times 10^{-12}$  for  $x = 3$ , and  $(2.34 \pm 0.25) \times 10^{-12}$   $\text{cm}^3 \text{ molecule}^{-1} \text{ s}^{-1}$  for  $x = 4$ . Although there is some evidence that  $k_5$  increases with increasing chain length, it can also be argued that there is no such effect since values for  $x = 1, 3$ , and  $4$  are indistinguishable within the combined experimental uncertainties. For simplicity, we choose to cite a final number for  $k_5$ , with error limits which encompass the extremes of the individual determinations; hence,  $k_5(\text{Cl} + \text{C}_x\text{F}_{2x+1}\text{CHO}) = (2.1 \pm 0.5) \times 10^{-12}$   $\text{cm}^3 \text{ molecule}^{-1} \text{ s}^{-1}$ .

Wallington and Hurley<sup>17</sup> report  $k(\text{Cl} + \text{CF}_3\text{CHO}) = (1.8 \pm 0.4) \times 10^{-12}$ , Sulbaek Andersen et al.<sup>8</sup> report  $k(\text{Cl} + \text{C}_2\text{F}_5\text{CHO}) = (1.96 \pm 0.28) \times 10^{-12}$ , and Hurley et al.<sup>10</sup> deduced  $k(\text{Cl} + \text{C}_x\text{F}_{2x+1}\text{CHO}) = (2.3 \pm 0.7) \times 10^{-12}$   $\text{cm}^3 \text{ molecule}^{-1} \text{ s}^{-1}$  for  $x = 1-4$  during a study of the Cl atom initiated oxidation of  $\text{C}_x\text{F}_{2x+1}\text{CH}_2\text{OH}$  alcohols. Data from Scollard et al.<sup>18</sup> have been rescaled to give  $k(\text{Cl} + \text{CF}_3\text{CHO}) = 2.28 \times 10^{-12}$   $\text{cm}^3 \text{ molecule}^{-1} \text{ s}^{-1}$ .<sup>19</sup> These values are indistinguishable from the value of  $k(\text{Cl} + \text{C}_x\text{F}_{2x+1}\text{CHO}, x = 1, 3, 4)$  reported herein.

$\text{CF}_3\text{CHO}$  and  $\text{C}_4\text{F}_9\text{CHO}$  are factors of 38<sup>20</sup> and 110<sup>21</sup> less reactive toward Cl atoms than their nonfluorinated counterparts  $\text{CH}_3\text{CHO}$  and  $\text{C}_4\text{H}_9\text{CHO}$ . Reaction of Cl atoms with  $\text{CH}_3\text{CHO}$  proceeds exclusively (>99%) via abstraction of the aldehydic hydrogen.<sup>22</sup> Upon the basis of recent results for similar aldehydes,<sup>23</sup> abstraction of the aldehydic hydrogen is also expected to play a major role in the reaction of Cl atoms with  $\text{C}_4\text{F}_9\text{CHO}$ . It is clear that  $\text{C}_x\text{F}_{2x+1}$  groups have a strong deactivating effect on the aldehydic functional group.

**3.2. Product Study of the Cl +  $\text{C}_x\text{F}_{2x+1}\text{CHO}$  ( $x = 1, 3, 4$ ) Reaction in the Presence of  $\text{NO}_x$  in 700 Torr of Air.** Experiments were performed to investigate the mechanism of Cl atom initiated oxidation of  $\text{C}_x\text{F}_{2x+1}\text{CHO}$  in the presence of  $\text{NO}_x$ . Mixtures containing 4.2–7.5 mTorr  $\text{C}_2\text{F}_5\text{CHO}$ , 150–194 mTorr  $\text{Cl}_2$ , 46–51 mTorr NO, and 9 Torr  $\text{O}_2$  in 700 Torr of  $\text{N}_2$  diluent were introduced into the reaction chamber and irradiated using the UV blacklamps. Figure 2 shows spectra acquired before (A) and after (B) a 131-s irradiation of a mixture of 7.47 mTorr  $\text{CF}_3\text{CHO}$ , 150 mTorr  $\text{Cl}_2$ , 51 mTorr NO, and 9 Torr  $\text{O}_2$  in 700 Torr of  $\text{N}_2$ . The consumption of  $\text{C}_2\text{F}_5\text{CHO}$  was 39%. Comparison of the IR features in panel B with the reference spectra of  $\text{COF}_2$  and  $\text{ClNO}$  given in panels C and D shows the formation of these species. Product features attributable to small amounts of  $\text{CF}_3\text{ONO}_2$  and  $\text{CF}_3\text{C}(\text{O})\text{OONO}_2$  were also detected.

Figure 3 shows the observed formation of  $\text{COF}_2$  versus loss of  $\text{C}_x\text{F}_{2x+1}\text{CHO}$  following UV irradiation of gas mixtures containing  $\text{CF}_3\text{CHO}$ ,  $\text{C}_3\text{F}_7\text{CHO}$ , and  $\text{C}_4\text{F}_9\text{CHO}$ , respectively, together with  $\text{Cl}_2$  and NO in 700 Torr of  $\text{O}_2/\text{N}_2$  diluent. The lines through the data in Figure 3 are linear least-squares fits (forced through zero) which give the following molar yields of  $\text{COF}_2$ :  $91 \pm 11\%$ ,  $x = 1$ ;  $273 \pm 36\%$ ,  $x = 3$ ; and  $371 \pm 44\%$ ,  $x = 4$ . Quoted errors are two standard deviations from the regression analysis, together with an additional 10% range to reflect uncertainties associated with calibration of the reference spectra. Small quantities (molar yields  $\leq 3\%$ ) of  $\text{CF}_3\text{ONO}_2$  and  $\text{C}_x\text{F}_{2x+1}\text{C}(\text{O})\text{O}_2\text{NO}_2$  were also detected in these experiments. Thus, we can account for  $(96 \pm 11)\%$  of the loss of  $\text{CF}_3\text{CHO}$ ,

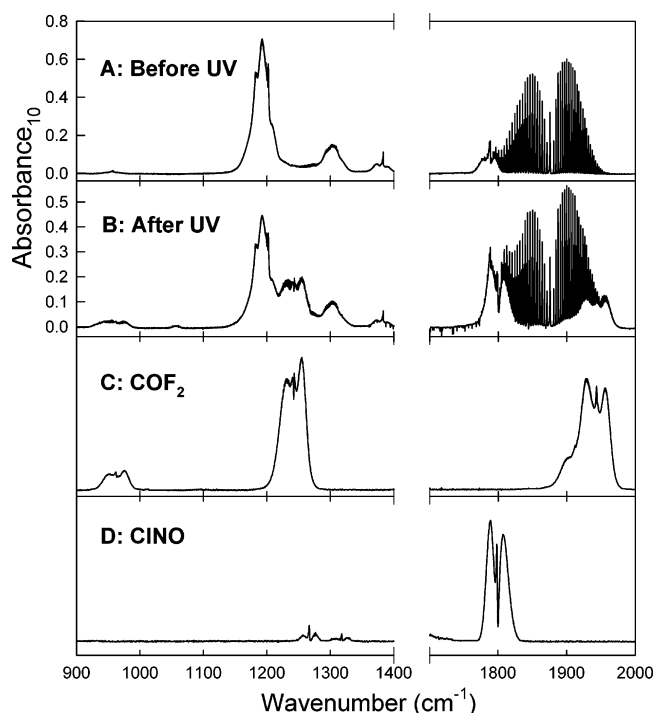
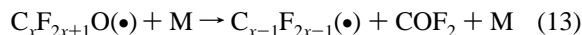
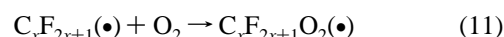
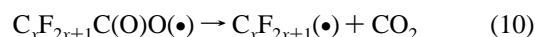
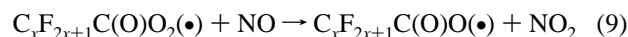
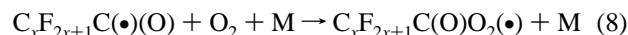
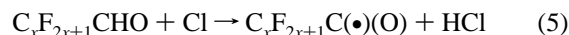


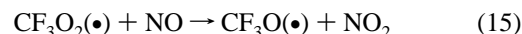
**Figure 2.** IR spectra obtained before (A) and after (B) a 131-s irradiation of a mixture of 7.47 mTorr  $\text{CF}_3\text{CHO}$ , 150 mTorr  $\text{Cl}_2$ , 51 mTorr NO, and 9 Torr  $\text{O}_2$  in 700 Torr of  $\text{N}_2$ . The consumption of  $\text{C}_2\text{F}_5\text{CHO}$  was 39%. Panels C and D are reference spectra of  $\text{COF}_2$  and  $\text{ClNO}$ , respectively.

$95 \pm 12\%$  of the loss of  $\text{C}_3\text{F}_7\text{CHO}$  and  $97 \pm 11\%$  of the loss of  $\text{C}_4\text{F}_9\text{CHO}$ .

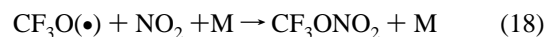
The simplest explanation for the observed product distribution is that reaction 5 is followed by (8–16):<sup>8</sup>



Repetition of reaction 11–13 results in the “unzipping” of the radical and the formation of  $x-1$  molecules of  $\text{COF}_2$  for  $\text{C}_x\text{F}_{2x+1}\text{CHO}$  ( $x = 1, 3, 4$ ). The last radical formed,  $\text{CF}_3$ , will be converted into  $\text{COF}_2$  by reactions 14–16:



$\text{NO}_2$  is formed during the reaction sequence given above. In the presence of  $\text{NO}_2$ ,  $\text{C}_x\text{F}_{2x+1}\text{C}(\text{O})\text{O}_2\text{NO}_2$  and  $\text{CF}_3\text{ONO}_2$  will be formed via reactions 17 and 18:



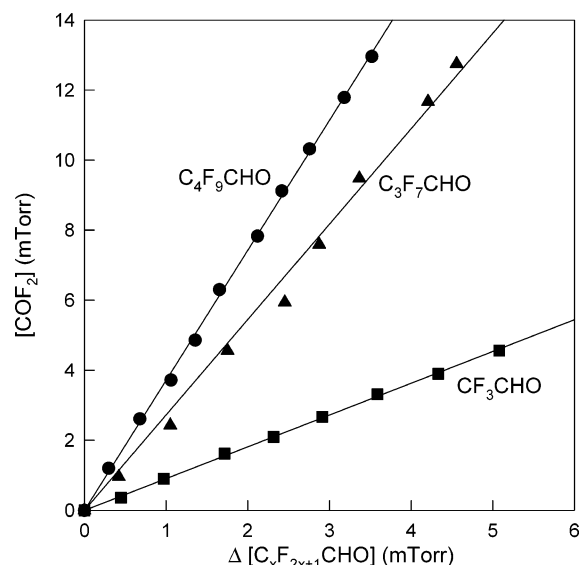
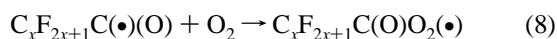
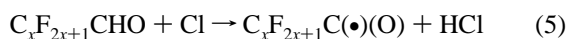


**Figure 3.** Yield of  $\text{COF}_2$  from the reaction of Cl atoms with  $\text{C}_x\text{F}_{2x+1}\text{CHO}$  in the presence of  $\text{NO}_x$  in 700 Torr of air. Circles, triangles, and squares indicate  $\text{COF}_2$  yield from  $\text{C}_4\text{F}_9\text{CHO}$ ,  $\text{C}_3\text{F}_7\text{CHO}$ , and  $\text{CF}_3\text{CHO}$ , respectively.

Using calibrated reference spectra of  $\text{C}_x\text{F}_{2x+1}\text{C(O)OH}$ , evidence for the formation of these species was sought in the product spectra, but not found. An upper limit for the molar formation of  $\text{C}_x\text{F}_{2x+1}\text{C(O)OH}$  of 2% was established.

**3.3. IR Spectra of  $\text{C}_x\text{F}_{2x+1}\text{C(O)O}_2\text{NO}_2$  ( $x = 1, 3, 4$ ).** To record the IR spectra of  $\text{C}_x\text{F}_{2x+1}\text{C(O)O}_2\text{NO}_2$  ( $x = 1, 3, 4$ ) mixtures of 3.9–8.3 mTorr  $\text{C}_x\text{F}_{2x+1}\text{CHO}$ , 90–202 mTorr  $\text{Cl}_2$ , and 10–12 mTorr  $\text{NO}_2$  in 700 Torr of  $\text{O}_2$  diluent were subjected to UV irradiation. The reaction of Cl atoms with  $\text{C}_x\text{F}_{2x+1}\text{CHO}$  will lead to the formation of  $\text{C}_x\text{F}_{2x+1}\text{C(O)O}_2$ . It is expected that the acyl peroxy radicals,  $\text{C}_x\text{F}_{2x+1}\text{C(O)O}_2$  ( $x = 1, 3, 4$ ), will react rapidly with  $\text{NO}_2$  to give the peroxy nitrates,  $\text{C}_x\text{F}_{2x+1}\text{C(O)O}_2\text{NO}_2$ :



Peroxy nitrates are thermally unstable and decompose to reform acetyl peroxy radicals and  $\text{NO}_2$ . It seems reasonable to assume that  $\text{C}_x\text{F}_{2x+1}\text{C(O)O}_2\text{NO}_2$  ( $x = 3, 4$ ) will decompose at a rate similar to that of  $\text{CF}_3\text{C(O)O}_2\text{NO}_2$  and hence will have a lifetime at 296 K of approximately 5 h.<sup>24</sup> In the presence of excess  $\text{NO}_2$  thermal decomposition of  $\text{C}_x\text{F}_{2x+1}\text{C(O)O}_2\text{NO}_2$  is masked by its reformation via reaction 17. Following UV irradiation of  $\text{C}_x\text{F}_{2x+1}\text{CHO}/\text{NO}_2/\text{Cl}_2/\text{O}_2$  mixtures three carbon-containing products were observed:  $\text{COF}_2$ ,  $\text{CO}_2$ , and a product with the IR features shown in panels A, B, and D of Figure 4. The features shown in Figure 4 increased linearly with loss of the parent compound. The product features at 790–792, 1301, 1761–1762, and 1848–1857  $\text{cm}^{-1}$  are characteristic of the  $\text{NO}_2$  deformation,  $\text{NO}_2$  symmetric stretch,  $\text{NO}_2$  asymmetric stretch, and CO stretching modes in acetyl peroxy nitrates. We assign the spectra in shown in panels A, B, and D of Figure 4 to  $\text{C}_4\text{F}_9\text{C(O)O}_2\text{NO}_2$ ,  $\text{C}_3\text{F}_7\text{C(O)O}_2\text{NO}_2$ , and  $\text{CF}_3\text{C(O)O}_2\text{NO}_2$ , respectively. For comparison, the spectra of  $\text{C}_2\text{F}_5\text{C(O)O}_2\text{NO}_2$ <sup>8</sup> and  $\text{CH}_3\text{C(O)O}_2\text{NO}_2$ <sup>25</sup> are also shown in Figure 4. Calibration of the spectra for  $\text{C}_x\text{F}_{2x+1}\text{C(O)O}_2\text{NO}_2$  ( $x = 1, 3, 4$ ) were achieved by assuming

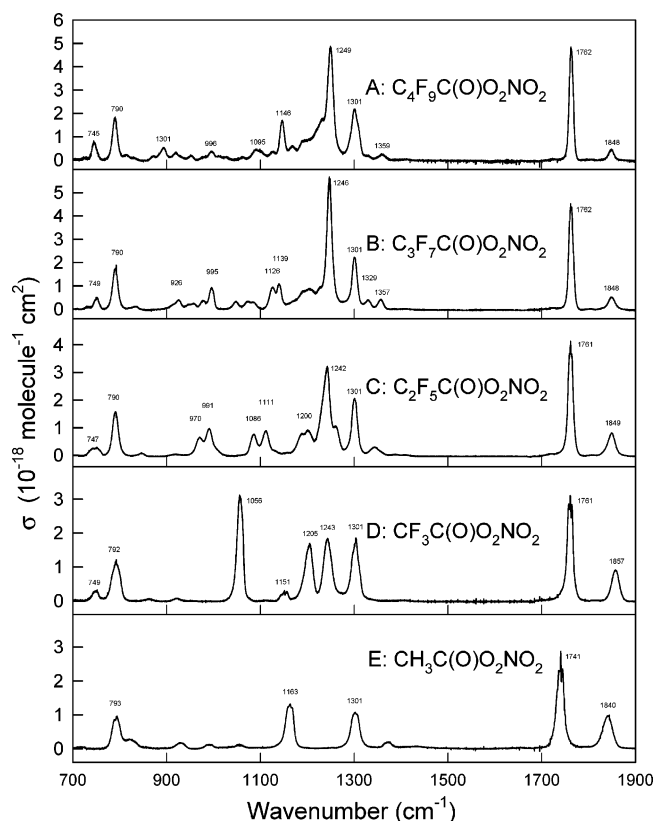


**Figure 4.** Infrared spectra of  $\text{C}_4\text{F}_9\text{C(O)O}_2\text{NO}_2$  (A),  $\text{C}_3\text{F}_7\text{C(O)O}_2\text{NO}_2$  (B),  $\text{C}_2\text{F}_5\text{C(O)O}_2\text{NO}_2$  (C),  $\text{CF}_3\text{C(O)O}_2\text{NO}_2$  (D), and  $\text{CH}_3\text{C(O)O}_2\text{NO}_2$ , PAN (E).

that reaction 5 leads to the formation of  $\text{C}_x\text{F}_{2x+1}\text{C(O)O}_2\text{NO}_2$  and  $\text{COF}_2$  in a combined molar carbon yield of 100%.

The integrated band strength (1700–1800  $\text{cm}^{-1}$ ) of the  $\text{NO}_2$  asymmetric stretching feature was  $(5.53 \pm 1.11) \times 10^{-17}$  for  $\text{C}_4\text{F}_9\text{C(O)O}_2\text{NO}_2$ ,  $(5.56 \pm 1.11) \times 10^{-17}$  for  $\text{C}_3\text{F}_7\text{C(O)O}_2\text{NO}_2$ , and  $(5.15 \pm 1.03) \times 10^{-17}$   $\text{cm molecule}^{-1}$  for  $\text{CF}_3\text{C(O)O}_2\text{NO}_2$  (we attribute 20% uncertainty to these measurements). These values are indistinguishable from those of  $(5.14 \pm 0.10) \times 10^{-17}$  and  $(5.25 \pm 1.04) \times 10^{-17}$   $\text{cm molecule}^{-1}$  for the corresponding features in  $\text{CH}_3\text{C(O)O}_2\text{NO}_2$ <sup>26</sup> and  $\text{C}_2\text{F}_5\text{C(O)O}_2\text{NO}_2$ .<sup>8</sup>

**3.4. Computational Results.** The B3LYP/6-311G(d,p) optimized geometries of (A)  $\text{CH}_3\text{C(O)O}_2\text{NO}_2$  and (B)  $\text{CF}_3\text{C(O)O}_2\text{NO}_2$  are shown in Figure 5. The optimizations indicate that these species may be characterized as complexes of carboxyl and  $\text{NO}_3$  radicals, e.g.,  $\text{CF}_3\text{C(O)O}_2\text{NO}_2$  is a  $\text{CF}_3\text{C(O)O} \cdots \text{O}_3\text{N}$  complex, the carbonyl oxygen bonds via an  $\text{sp}^3$  hybrid orbital to the  $\text{NO}_3$  oxygen, which bonds via an  $\text{sp}^2$  hybrid orbital. Tables 1 and 2 list the computed IR spectra of these compounds between 700 and 1900  $\text{cm}^{-1}$ . Calculated vibrational frequencies were scaled by the empirical factor of 0.9614 parametrized for B3LYP/6-31G(d) by Scott and Radom,<sup>27</sup> and the results are presented in Tables 1 and 2. Comparison of the data in Tables 1 and 2 with the spectra in Figure 4 reveals that the computations produce scaled frequencies which are generally in good agreement (within 10  $\text{cm}^{-1}$ ) of the experimental results. However, discrepancies between theory and experiment of up to approximately 66  $\text{cm}^{-1}$  are evident for some features.

The B3LYP/6-311G(d,p) geometry optimizations of  $\text{C}_2\text{F}_5\text{C(O)O}_2\text{NO}_2$  locate three conformers **I**, **II**, and **III**, as displayed in Figure 6. The B3LYP/6-311G(d,p) energies of **II** and **III**, relative to **I**, are 0.50, and  $-0.13$  kcal/mol, respectively. Inclusion of zero-point energy does not alter these relative energies significantly. In light of these small energy differences,

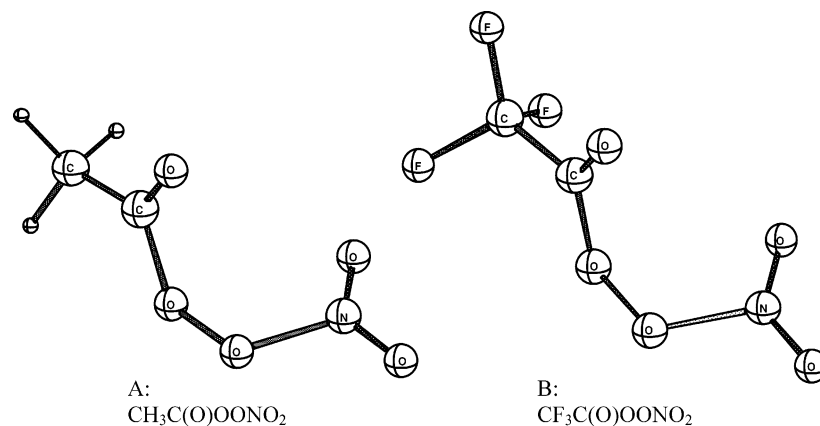


**Figure 5.** B3LYP/6-311G(d,p) structures of (A)  $\text{CH}_3\text{C}(\text{O})\text{OONO}_2$  and (B)  $\text{CF}_3\text{C}(\text{O})\text{OONO}_2$ .

**TABLE 1: B3LYP/6-311G(d,p) Vibrational Frequencies of  $\text{CH}_3\text{C}(\text{O})\text{OONO}_2$  between 700 and 1900  $\text{cm}^{-1}$ <sup>a</sup>**

frequency	IR intensity
697	11.1
700	1.8
779	208.9
797	58.7
939	14.4
966	26.3
1019	0.1046
1123	241
1310	250.51
1344	33.3
1413	10.7
1418	11.3
1761	398
1822	218.3

<sup>a</sup> Scaled frequencies are in  $\text{cm}^{-1}$  and computed IR intensities are in  $\text{km/mol}$ .

**TABLE 2: B3LYP/6-311G(d,p) Vibrational Frequencies of  $\text{CF}_3\text{C}(\text{O})\text{OONO}_2$  between 700 and 1900  $\text{cm}^{-1}$ <sup>a</sup>**

frequency	IR intensity
688	11.2
720	22.4
739	7.7
782	210.3
841	15.09
932	13.5
1012	445.3
1139	272.6
1182	302.8
1242	63.4
1311	263.37
1786	384.7
1839	210.4

<sup>a</sup> Scaled frequencies are in  $\text{cm}^{-1}$  and computed IR intensities are in  $\text{km/mol}$ .

the conformers should be present in approximately equal amounts. Scaled vibrational frequencies between 700 and approximately 1900  $\text{cm}^{-1}$  are listed in Table 3. Generally, there is little deviation in the frequency of any particular mode between the three conformers. This does not hold in every case, however. Experimental peaks at 1086 and 1111  $\text{cm}^{-1}$  are assigned to one mode where the deviation of frequencies between **II** and **III** is  $\sim 27 \text{ cm}^{-1}$ , while the broad peak at 1242  $\text{cm}^{-1}$  may be the result of two or even three vibrational modes. Agreement between experiment and the scaled B3LYP frequencies is in general good, with the largest discrepancies being approximately 40  $\text{cm}^{-1}$ .

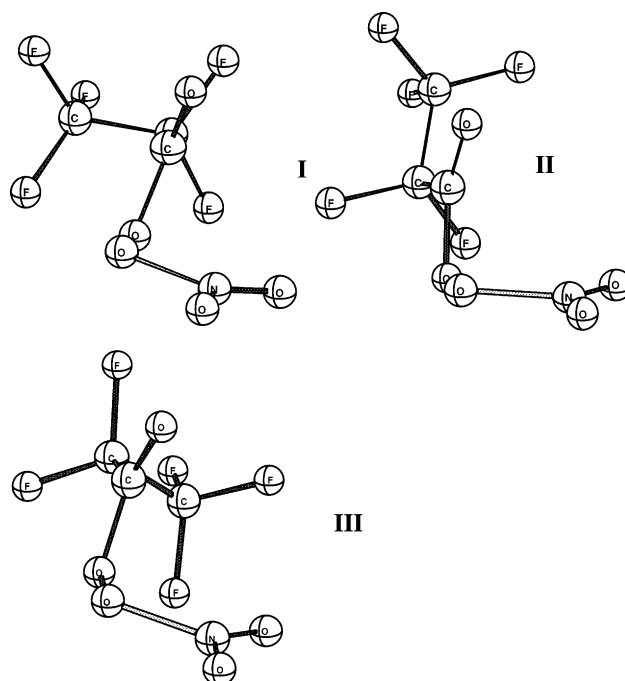
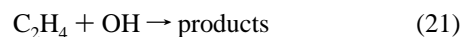
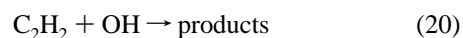
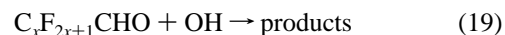


**Figure 6.** B3LYP/6-311G(d,p) optimized conformers **I**, **II**, and **III** of  $\text{C}_2\text{F}_5\text{C}(\text{O})\text{OONO}_2$ .

As discussed above, typically there was little variation in the frequency of a given mode between the **I**, **II**, and **III** conformers of  $\text{C}_2\text{F}_5\text{C}(\text{O})\text{OONO}_2$ .  $\text{C}_3\text{F}_7\text{C}(\text{O})\text{OONO}_2$  and  $\text{C}_4\text{F}_9\text{C}(\text{O})\text{OONO}_2$  were optimized only in conformers corresponding to analogues of **I**. Table 4 shows the scaled frequencies and IR intensities. Discrepancies between theory and experiment are small, with the largest deviations being approximately 40  $\text{cm}^{-1}$ .

**3.5. Relative Rate Study of the  $\text{OH} + \text{C}_x\text{F}_{2x+1}\text{CHO}$  ( $x = 1, 3, 4$ ) Reaction in 700 Torr of Air.** The kinetics of reaction 19 were measured relative to reactions 20 and 21:



Initial reactant concentrations were 16.2–31.0 mTorr of  $\text{C}_x\text{F}_{2x+1}\text{CHO}$ , 139–176 mTorr of  $\text{CH}_3\text{ONO}$ , 10.8–17.9 mTorr  $\text{NO}$ , and 3.07–8.25 mTorr of either  $\text{C}_2\text{H}_2$  or  $\text{C}_2\text{H}_4$  in 700 Torr of air diluent. When working with compounds such as  $\text{C}_x\text{F}_{2x+1}\text{CHO}$  which have modest reactivity toward  $\text{OH}$  radicals and poorly

**TABLE 3: B3LYP/6-311G(d,p) Vibrational Frequencies of C<sub>2</sub>F<sub>5</sub>C(O)OONO<sub>2</sub> between 700 and 1900 cm<sup>-1a</sup>**

I	I	II	II	III	III
frequency	IR intens	frequency	IR intens	frequency	IR intens
688	11	688	12	687	9
715	29	718	44	711	28
727	4	736	5	728	4
781	223	781	221	781	196
827	16	829	17	825	19
927	4	901	169	929	16
958	308	947	245	957	245
1059	167	1084	120	1060	237
1140	155	1111	127	1139	142
1158	151	1170	218	1158	138
1171	357	1182	288	1172	352
1203	157	1195	90	1202	153
1272	112	1288	180	1272	96
1311	245	1314	203	1311	256
1787	386	1787	389	1785	395
1835	208	1826	195	1835	212

<sup>a</sup> Data are displayed for conformers I, II, and III. Scaled frequencies are in cm<sup>-1</sup>, and computed IR are in km/mol.

**TABLE 4: Scaled B3LYP/6-311G(d,p) Vibrational Frequencies of C<sub>3</sub>F<sub>7</sub>C(O)OONO<sub>2</sub> and C<sub>4</sub>F<sub>9</sub>C(O)OONO<sub>2</sub> between 700 and 1900 cm<sup>-1a</sup>**

C <sub>3</sub> F <sub>7</sub> C(O)OONO <sub>2</sub>		C <sub>4</sub> F <sub>9</sub> C(O)OONO <sub>2</sub>	
frequency	IR intens	frequency	IR intens
688	10	689.04	10.8
707	40	699.25	58.03
724	14	720.67	10.3
781	240	779.42	277.9
814	30	794.77	27.1
888	133	847.70	46.1
929	48	927.99	27.2
1025	111	989.88	90
1089	254	1050.90	153.9
1130	79	1098.59	213.1
1135	144	1121.23	37.5
1147	53	1122.91	78.2
1170	212	1134.64	76.7
1187	434	1158.01	197
1228	91	1174.35	229.3
1291	73	1185.56	428.31
1311	264	1199.41	138.1
1787	388	1243.99	50.3
1836	208	1296.53	72.7
		1311.33	258.8
		1786.99	389
		1836.37	207.3

<sup>a</sup> Frequencies are in cm<sup>-1</sup> and computed IR intensities are in km/mol.

defined (broad) IR features, an indirect variation of the relative rate technique can be useful.<sup>13</sup> As discussed above, in the presence of excess NO the oxidation of C<sub>x</sub>F<sub>2x+1</sub>CHO gives COF<sub>2</sub> and C<sub>x</sub>F<sub>2x+1</sub>ONO<sub>2</sub> in essentially quantitative yield. COF<sub>2</sub> and CF<sub>3</sub>ONO<sub>2</sub> have intense characteristic IR features that are convenient to monitor. In the present work for *x* = 3 and 4, the loss of C<sub>x</sub>F<sub>2x+1</sub>CHO was inferred by the formation of its oxidation products COF<sub>2</sub> and CF<sub>3</sub>ONO<sub>2</sub>; for *x* = 1 the loss was measured directly. We assume that the reaction of OH radicals with C<sub>x</sub>F<sub>2x+1</sub>CHO proceeds exclusively by hydrogen atom abstraction from the CHO group.

The calculated loss of C<sub>x</sub>F<sub>2x+1</sub>CHO versus that of the reference compounds in the presence of OH atoms is shown in Figure 7. Linear least-squares analysis of the data in Figure 5 gives  $k_{19}/k_{20} = 0.728 \pm 0.095$  and  $k_{19}/k_{21} = 0.0813 \pm 0.0095$ , where the quoted uncertainties are two standard deviations from the linear regressions together with our estimation of the

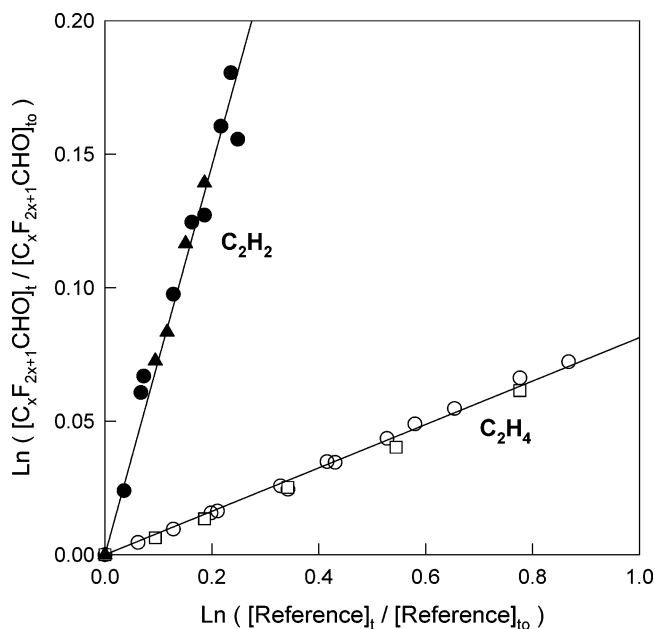


**Figure 7.** Decay of CF<sub>3</sub>CHO (triangles), C<sub>3</sub>F<sub>7</sub>CHO (squares), and C<sub>4</sub>F<sub>9</sub>CHO (circles) versus C<sub>2</sub>H<sub>4</sub> (open symbols) or C<sub>2</sub>H<sub>2</sub> (solid symbols) in the presence of OH radicals in 700 Torr of air diluent at 296 ± 2 K. Loss of CF<sub>3</sub>CHO decay was measured directly, and loss of C<sub>3</sub>F<sub>7</sub>CHO and C<sub>4</sub>F<sub>9</sub>CHO was measured indirectly; see text for details.

uncertainties associated with the IR analysis of the reactant and reference concentrations. Using  $k_{20} = 8.45 \times 10^{-13}$ ,<sup>28</sup> and  $k_{21} = 8.52 \times 10^{-12}$ ,<sup>29</sup> we derive  $k_{19} = (6.15 \pm 0.80) \times 10^{-13}$ , and  $k_{19} = (6.93 \pm 0.81) \times 10^{-13}$  cm<sup>3</sup> molecule<sup>-1</sup> s<sup>-1</sup>. We choose to quote a final value for  $k_4$  which is the average of those determined using the two reference compounds together with error limits which encompass the extremes of the individual determinations; hence,  $k_{19} = (6.5 \pm 1.2) \times 10^{-13}$  cm<sup>3</sup> molecule<sup>-1</sup> s<sup>-1</sup>. While there are no previous studies of the reactivity of OH radicals toward C<sub>3</sub>F<sub>7</sub>CHO and C<sub>4</sub>F<sub>9</sub>CHO, we can compare our results with literature values for *x* = 1 and 2. Dóbé et al.<sup>30</sup> have measured  $k(\text{OH} + \text{CF}_3\text{CHO}) = (1.1 \pm 0.7) \times 10^{-12}$  cm<sup>3</sup> molecule<sup>-1</sup> s<sup>-1</sup> using discharge flow techniques. Scollard et al.<sup>18</sup> have reported  $k(\text{OH} + \text{CF}_3\text{CHO}) = (6.5 \pm 0.5) \times 10^{-13}$  and  $(5.4 \pm 1.2) \times 10^{-13}$  cm<sup>3</sup> molecule<sup>-1</sup> s<sup>-1</sup> based on pulsed laser photolysis resonance fluorescence and relative rate experiments, respectively. Sellevåg et al.<sup>19</sup> report  $k(\text{OH} + \text{CF}_3\text{CHO})/k(\text{OH} + \text{C}_2\text{H}_6) = 2.00$ , which, using  $k(\text{OH} + \text{C}_2\text{H}_6) = 2.4 \times 10^{-13}$ ,<sup>20</sup> gives  $k(\text{OH} + \text{CF}_3\text{CHO}) = 4.8 \times 10^{-13}$  cm<sup>3</sup> molecule<sup>-1</sup> s<sup>-1</sup>. Andersen et al.<sup>8</sup> report  $k(\text{OH} + \text{C}_2\text{F}_5\text{CHO}) = (5.26 \pm 0.80) \times 10^{-13}$  cm<sup>3</sup> molecule<sup>-1</sup> s<sup>-1</sup>. The IUPAC data evaluation committee recommends  $k(\text{OH} + \text{CF}_3\text{CHO}) = (6.0 \pm 1.2) \times 10^{-13}$  cm<sup>3</sup> molecule<sup>-1</sup> s<sup>-1</sup> at 298 K. The reactivity of C<sub>x</sub>F<sub>2x+1</sub>CHO (*x* = 1, 3, 4) toward OH radicals measured in the present work is indistinguishable, within the likely experimental uncertainties, from that reported previously for CF<sub>3</sub>CHO and C<sub>2</sub>F<sub>5</sub>CHO.

#### 4. Implications for Atmospheric Chemistry

The present work improves our understanding of the atmospheric chemistry of perfluorinated aldehydes of the general formula C<sub>x</sub>F<sub>2x+1</sub>CHO. Cl atoms and OH radicals react with C<sub>x</sub>F<sub>2x+1</sub>CHO (*x* = 1, 3, 4) with rate constants of  $(2.1 \pm 0.5) \times 10^{-12}$  and  $(6.5 \pm 1.2) \times 10^{-13}$  cm<sup>3</sup> molecule<sup>-1</sup> s<sup>-1</sup>, respectively. Reaction occurs exclusively at the aldehydic hydrogen atom. Given the finding in the present work that the reactivity of Cl atoms and OH radicals toward CF<sub>3</sub>CHO, C<sub>3</sub>F<sub>7</sub>CHO, and C<sub>4</sub>F<sub>9</sub>

CHO are indistinguishable, it seems reasonable to generalize our results to all members of the  $\text{C}_x\text{F}_{2x+1}\text{CHO}$  series.

The value of  $k(\text{OH} + \text{C}_x\text{F}_{2x+1}\text{CHO})$  derived above can be used to provide an estimate of the atmospheric lifetime of  $\text{C}_x\text{F}_{2x+1}\text{CHO}$  with respect to reaction with OH radicals. Using the 296 K rate constant measured here together with a global weighted-average OH concentration of  $1.0 \times 10^6$  molecule  $\text{cm}^{-3}$ <sup>31</sup> leads to an estimated atmospheric lifetime of  $\text{C}_x\text{F}_{2x+1}\text{CHO}$  of 18 days.

The approximate nature of this atmospheric lifetime estimate should be stressed. The average daily concentration of OH radicals in the atmosphere varies significantly with both location and season.<sup>32</sup> The estimate presented here represents the global average lifetime with respect to reaction with OH radicals.

Reaction of OH radicals with  $\text{C}_x\text{F}_{2x+1}\text{CHO}$  proceeds via hydrogen atom abstraction to give  $\text{C}_x\text{F}_{2x+1}\text{C}(\bullet)(\text{O})$  radicals. The atmospheric fate of  $\text{C}_x\text{F}_{2x+1}\text{C}(\bullet)(\text{O})$  radicals is addition of  $\text{O}_2$  to give the corresponding acyl peroxy radicals. As discussed in sections 3.3 and 3.4, in the presence of excess  $\text{NO}_2$  the fate of the acyl peroxy radicals is addition of  $\text{NO}_2$  to give the thermally unstable peroxy nitrates,  $\text{C}_x\text{F}_{2x+1}\text{C}(\text{O})\text{O}_2\text{NO}_2$ . As discussed in section 3.2, in the presence of excess NO the fate of the acyl peroxy radicals is reaction to give acetoxy radicals,  $\text{C}_x\text{F}_{2x+1}\text{C}(\text{O})\text{O}(\bullet)$ , which will eliminate  $\text{CO}_2$  and initiate a sequence of reactions in which the molecule “unzips” via shedding  $\text{COF}_2$  units. No evidence for the formation of perfluorocarboxylic acids was found in the present experiments. On the basis of the results reported here and elsewhere,<sup>8</sup> we conclude that the OH radical initiated gas-phase atmospheric oxidation of  $\text{C}_x\text{F}_{2x+1}\text{CHO}$  in the presence of excess NO is not a significant source of perfluorocarboxylic acids,  $\text{C}_x\text{F}_{2x+1}\text{C}(\text{O})\text{OH}$ . However, it should be noted that in absence of  $\text{NO}_x$ , perfluorocarboxylic acid formation is observed during the Cl atom initiated oxidation of  $\text{C}_x\text{F}_{2x+1}\text{CHO}$  ( $x = 1-4$ ), presumably as a result of reactions of  $\text{C}_x\text{F}_{2x+1}\text{C}(\text{O})\text{O}_2$  with  $\text{HO}_2$  radicals.<sup>9,10</sup>

At this point it is germane to note that, in addition to reaction with OH radicals, other loss mechanisms (e.g., photolysis and hydrate formation) for  $\text{C}_x\text{F}_{2x+1}\text{CHO}$  need to be considered.  $\text{C}_x\text{F}_{2x+1}\text{CHO}$  ( $x = 1-3$ ,<sup>33-36</sup>) absorb at wavelengths  $> 300$  nm, where the solar flux in the troposphere is substantial.<sup>2</sup> Rattigan et al.<sup>37</sup> conducted a modeling study, assumed a photodissociation yield of unity, and calculated a lifetime of  $\text{CF}_3\text{CHO}$  with respect to photolysis of 4 h (30°N and 8.75 km altitude). Longer chain members of the  $\text{C}_x\text{F}_{2x+1}\text{CHO}$  series absorb more strongly<sup>34,36</sup> and may photolyze more rapidly than  $\text{CF}_3\text{CHO}$ . Sellevåg et al.<sup>19</sup> conducted an experimental study and reported an upper limit of 0.02 for the effective quantum yield of photolysis of  $\text{CF}_3\text{CHO}$  in natural sunlight over the wavelength range 290–400 nm and a lower limit of 26 days for the lifetime of  $\text{CF}_3\text{CHO}$ . This result can be contrasted with the finding by Dodd and Smith<sup>38</sup> of a photodissociation quantum yield of 0.13 for  $\text{CF}_3\text{CHO}$  at 313 nm. As discussed by Sellevåg et al.,<sup>19</sup> the different photodissociation quantum yields may reflect the fact that the intensity of sunlight drops rapidly at wavelengths below 320 nm. Alternatively, there may be a discrepancy between the results reported in the two studies.

It is well established that  $\text{C}_x\text{F}_{2x+1}\text{CHO}$  form stable hydrates,  $\text{C}_x\text{F}_{2x+1}\text{C}(\text{OH})_2\text{H}$ . In fact, the aldehydes  $\text{C}_x\text{F}_{2x+1}\text{CHO}$  ( $x = 1-4$ ) are only available commercially in their hydrated form. Given the abundance of water (gas, liquid, and solid) in the environment and the relatively long lifetime (approximately 18 days) of  $\text{C}_x\text{F}_{2x+1}\text{CHO}$  with respect to reaction with OH radicals it seems reasonable to postulate that hydration may be a significant atmospheric loss of  $\text{C}_x\text{F}_{2x+1}\text{CHO}$ . Unfortunately, there are no

kinetic data available with which to compute the importance of hydration as an atmospheric loss mechanism for  $\text{C}_x\text{F}_{2x+1}\text{CHO}$ .

While the present work improves our understanding of the atmospheric chemistry of  $\text{C}_x\text{F}_{2x+1}\text{CHO}$  and their likely contribution to perfluorinated carboxylic acid pollution many uncertainties remain. Not least of which being the following: (i) the rate and mechanism of photolysis, (ii) the rate and mechanism of  $\text{C}_x\text{F}_{2x+1}\text{C}(\text{O})\text{O}_2(\bullet) + \text{HO}_2$  reactions, and (iii) the rate of hydration and fate of any hydrates formed.

**Acknowledgment.** M.P.S.A. thanks the Danish Research Agency for a research grant and Dean Sengupta (College of Engineering and Computer Science, University of Michigan – Dearborn) for helpful comments. J.E.S. thanks the National Center for Supercomputing Applications (Grant No. CHE010014N) and the Petroleum Research Fund (Grant No. 37058-GB6) for support. This research was funded, in part, by an NSERC Strategic Grant.

## References and Notes

- (1) Kissa, E. In *Fluorinated Surfactants, Synthesis, Properties, and Applications*; Schick, M. J., Fowkes, F. M., Eds.; Marcel Dekker: New York, 1994.
- (2) Atkinson, R.; Cox, R. A.; Lesclaux, R.; Niki, H.; Zellner, R. Degradation Mechanisms, In *Scientific Assessment of Stratospheric Ozone*, Global Ozone research and Monitoring Project - Report No. 20; World Meteorological Organization: Geneva, Switzerland, 1989; Vol. 2.
- (3) Moody, C. A.; Martin, J. W.; Kwan, W. C.; Muir, D. C. G.; Mabury, S. A. *Environ. Sci. Technol.* **2002**, *36*, 545.
- (4) Moody, C. A.; Kwan, W. C.; Martin, J. W.; Muir, D. C. G.; Mabury, S. A. *Anal. Chem.* **2001**, *73*, 2200.
- (5) Martin, J. W.; Smithwick, M. M.; Braune, B. M.; Hoekstra, P. F.; Muir, D. C. G.; Mabury, S. A. *Environ. Sci. Technol.* **2004**, *38*, 373.
- (6) *Determination of Low Levels of Fluoropolymer Polymerization Aids—A Guidance Document*; The Society of the Plastics Industry, SPI Literature Catalogue # BZ-102, New York, 2003.
- (7) Ellis, D. A.; Mabury, S. A.; Martin, J. W.; Muir, D. C. G. *Nature* **2001**, *412*, 6844.
- (8) Sulbaek Andersen, M. P.; Hurley, M. D.; Wallington, T. J.; Ball, J. C.; Martin, J. W.; Ellis, D. A.; Mabury, S. A.; Nielsen, O. J. *Chem. Phys. Lett.* **2003**, *379*, 28.
- (9) Sulbaek Andersen, M. P.; Hurley, M. D.; Wallington, T. J.; Ball, J. C.; Martin, J. W.; Ellis, D. A.; Mabury, S. A. *Chem. Phys. Lett.* **2003**, *381*, 14.
- (10) Hurley, M. D.; Wallington, T. J.; Sulbaek Andersen, M. P.; Ellis, D. A.; Martin, J. W.; Mabury, S. A. *J. Phys. Chem. A* **2004**, *108*, 1973.
- (11) Hurley, M. D.; Sulbaek Andersen, M. P.; Wallington, T. J.; Ellis, D. A.; Martin, J. W.; Mabury, S. A. *J. Phys. Chem. A* **2004**, *108*, 615.
- (12) Wallington, T. J.; Japar, S. M. *J. Atmos. Chem.* **1989**, *9*, 399.
- (13) Takahashi, K.; Matsumi, Y.; Wallington, T. J.; Hurley, M. D. *J. Geophys. Res.* **2002**, *107*, ACH 4–1.
- (14) Frisch, M. J.; Trucks, G. W.; Schlegel, H. B.; Scuseria, G. E.; Robb, M. A.; Cheeseman, J. R.; Zakrzewski, V. G.; Montgomery, J. A., Jr.; Stratmann, R. E.; Burant, J. C.; Dapprich, S.; Millam, J. M.; Daniels, A. D.; Kudin, K. N.; Strain, M. C.; Farkas, O.; Tomasi, J.; Barone, V.; Cossi, M.; Cammi, R.; Mennucci, B.; Pomelli, C.; Adamo, C.; Clifford, S.; Ochterski, J.; Petersson, G. A.; Ayala, P. Y.; Cui, Q.; Morokuma, K.; Malick, D. K.; Rabuck, A. D.; Raghavachari, K.; Foresman, J. B.; Cioslowski, J.; Ortiz, J. V.; Stefanov, B. B.; Liu, G.; Liashenko, A.; Piskorz, P.; Komaromi, I.; Gomperts, R.; Martin, R. L.; Fox, D. J.; Keith, T.; Al-Laham, M. A.; Peng, C. Y.; Nanayakkara, A.; Gonzalez, C.; Challacombe, M.; Gill, P. M. W.; Johnson, B.; Chen, W.; Wong, M. W.; Andres, J. L.; Gonzalez, C.; Head-Gordon, M.; Replogle, E. S.; Pople, J. A. *Gaussian 98*, revision A.1, Gaussian, Inc.: Pittsburgh, PA, 1998.
- (15) Wine, P. H.; Semmes, D. H. *J. Phys. Chem.* **1983**, *87*, 3572.
- (16) Sander, S. P.; Friedl, R. R.; Golden, D. M.; Kurylo, M. J.; Huie, R. E.; Orkin, V. L.; Moortgat, G. K.; Ravishankara, A. R.; Kolb, C. E.; Molina, M. J.; Finlayson-Pitts, B. J. *J. JPL Publ.* 02-25, **2003**.
- (17) Wallington, T. J.; Hurley, M. D. *Int. J. Chem. Kinet.* **1993**, *25*, 819.
- (18) Scollard, D. J.; Treacy, J. J.; Sidebottom, H. W.; Balestra-Garcia, C.; Laverdet, G.; LeBras, G.; MacLeod, H.; Téton, S. *J. Phys. Chem.* **1993**, *97*, 4683.

- (19) Sellevåg, S. R.; Kelly, T.; Sidebottom, H.; Nielsen, C. J. *Phys. Chem. Chem. Phys.* **2004**, *6*, 1243.
- (20) Atkinson, R.; Baulch, D. L.; Cox, R. A.; Crowley, J. N.; Hampson, R. F., Jr.; Kerr, J. A.; Rossi, M. J.; Troe, J. *Summary of Evaluated Kinetic and Photochemical Data for Atmospheric Chemistry*; <http://www.iupac-kinetic.ch.cam.ac.uk> (Accessed Mar 2004).
- (21) Thevenet, R.; Mellouki, A.; Le Bras, G. *Int. J. Chem. Kinet.* **2000**, *32*, 676.
- (22) Niki, H.; Maker, P. D.; Savage, C. M.; Breitenbach, L. P. *J. Phys. Chem.* **1985**, *89*, 588.
- (23) Le Crâne, J.-P.; Villenave, E.; Hurley, M. D.; Wallington, T. J.; Nishida, S.; Takahashi, K.; Matsumi, Y. *J. Phys. Chem. A* **2004**, *108*, 795.
- (24) Wallington, T. J.; Sehested, J.; Nielsen, O. J. *Chem. Phys. Lett.* **1994**, *226*, 563.
- (25) Caralp, F.; Foucher, V.; Lesclaux, R.; Wallington, T. J.; Hurley, M. D. *Phys. Chem. Chem. Phys.* **1999**, *1*, 3509.
- (26) Tsalkani, N.; Toupance, G. *Atmos. Environ.* **1989**, *23*, 1849.
- (27) Scott, A. P.; Radom, L. *J. Phys. Chem.* **1996**, *100*, 16502.
- (28) Sørensen, M.; Kaiser, E. W.; Hurley, M. D.; Wallington, T. J.; Nielsen, O. J. *Int. J. Chem. Kinet.* **2003**, *35*, 191.
- (29) Calvert, J. G.; Atkinson, R.; Kerr, J. A.; Madronich, S.; Moortgat, G. K.; Wallington, T. J.; Yarwood, G. *The Mechanism of Atmospheric Oxidation of the Alkenes*; Oxford University Press: New York, 2000.
- (30) Dobe, S.; Kachatryan, L. A.; Berces, T. *Ber. Bunsen-Ges. Phys. Chem.* **1989**, *93*, 847.
- (31) Prinn, R. G.; Huang, J.; Weiss, R. F.; Cunnold, D. M.; Fraser, P. J.; Simmonds, P. G.; McCulloch, A.; Salameh, P.; O'Doherty, S.; Wang, R. H. J.; Porter, L.; Miller, B. R. *Science* **2001**, *292*, 1882.
- (32) Klečka, G.; Boethling, R.; Franklin, J.; Grady, L.; Howard, P. H.; Kannan, K.; Larson, R. J.; Mackay, D.; Muir, D.; van de Meent, D. *Evaluation of Persistence and Long-Range Transport of Organic Chemicals in the Environment*; SETAC Press: Pensacola, FL, 2000; p 45.
- (33) Meller, R.; Boglu, D.; Moortgat, G. K. *STEP-HALOCSIDE/AFEAS Workshop*; Dublin, Ireland, 23–25 March 1993; pp 130–138.
- (34) Borkowski, R. P.; Ausloss, P. *J. Am. Chem. Soc.* **1962**, *84*, 4044.
- (35) Lucazeau, G.; Sandorfy, C. *J. Mol. Spectrosc.* **1970**, *35*, 214.
- (36) Pritchard, G. O.; Miller, G. H.; Foote, J. K. *Can. J. Chem.* **1962**, *40*, 1830.
- (37) Rattigan, O. V.; Wild, O.; Cox, R. A. *J. Photochem. Photobiol. A: Chem.* **1998**, *112*, 1.
- (38) Dodd, R. E.; Smith, J. W. *J. Chem. Soc.* **1957**, 1465.